Accepted Manuscript

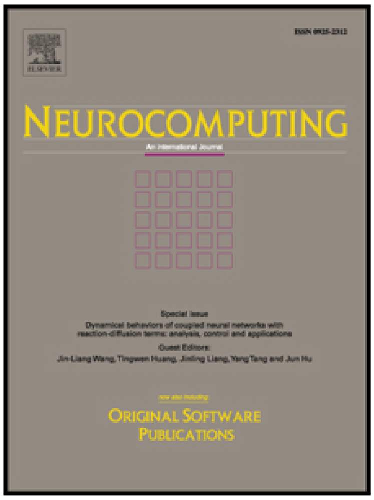

EEG Model Stability and Online Decoding of Attentional Demand during Gait using Gamma Band Features

A. Costa-García, E. Iáñez, A.J Del-Ama, Á. Gil-Águdo, J.M. Azorín

PII: S0925-2312(19)30848-3
DOI: https://doi.org/10.1016/j.neucom.2019.06.021
Reference: NEUCOM 20904

To appear in: *Neurocomputing*

Received date: 6 September 2018
Revised date: 13 April 2019
Accepted date: 7 June 2019

Please cite this article as: A. Costa-García, E. Iáñez, A.J Del-Ama, Á. Gil-Águdo, J.M. Azorín, EEG Model Stability and Online Decoding of Attentional Demand during Gait using Gamma Band Features, *Neurocomputing* (2019), doi: https://doi.org/10.1016/j.neucom.2019.06.021

EEG Model Stability and Online Decoding of Attentional Demand during Gait using Gamma Band Features

A. Costa-García[a], E. Iáñez[a,*], A. J Del-Ama[b], Á. Gil-Águdo[b], J. M. Azorín[a]

[a]Brain-Machine Interface Systems Lab, Systems Engineering and Automation Department, Miguel Hernández University of Elche, UMH, Avda. de la Universidad s/n. Ed. Innova, 03202, Elche, Spain

[b]Biomechanics and Technical Aids Units, Physical Medicine and Rehabilitation Department, National Hospital for Spinal Cord Injury, SESCAM, Finca de la Peraleda S/N, 45071, Toledo, Spain.

Abstract

Rehabilitation therapies are evolving oriented to improve their performances in terms of functional recovery. To achieve such recovery, the patients' involvement is an important factor that correlates with the plastic properties of the brain. By evaluating electroencephalographic signals, it is possible to modify, in real time, the parameters of the rehabilitation according to the patients' cognitive state. In this paper, an online brain-machine interface to measure the attention level during gait is presented. The system is based on the measurement of selective attention mechanisms manifested as power synchronization and desynchronization in the gamma band. A Linear Discriminant Analysis classifier is used to provide an attention index between 0 and 1 in real time. Robust techniques for artifact rejection and signal standardization are used in order to deal with the problems associated to the measurement of cortical signals during walking. The final interface is validated with 4 incomplete Spinal Cord Injury patients and 4 healthy participants. The system shows an average success rate of 68.1% in the classification of 3 attention levels and a stable behavior of these results during time.

*Corresponding author
Email address: eianez@umh.es (E. Iáñez)
URL: bmi.umh.es (E. Iáñez)

Keywords: attention level, gait, EEG, online
2018 MSC: 00-01, 99-00

1. Introduction

According to the World Health Organization (WHO), between 250 and 500 thousand people suffer a Spinal Cord Injury (SCI) every year [1]. These injuries refer to damages in the spinal cord resulting from trauma like traffic crashes, falls and violence. For that reason, young people, between 15 and 30 years, are more prone to suffer them. From a physical and cortical point of view, these people are more likely to recover mobility after rehabilitation [2]. In this sense, rehabilitation therapies have become a broad and current interest in science emerging from the social concern for the increasing number of people suffering this condition [3, 4, 5].

According to the concept of neuroplasticity, a wide range of experiences promote changes of the brain structure at a physical level both in humans [6] and animals [7]. It has been hypothesized that neuroplasticity could help rehabilitation performance following SCI by restoring and creating neural paths that compensate the lost functionalities [8, 9]. In fact, several studies proved an increase in plastic changes associated with higher levels of patients involvement during therapies [10, 11, 12].

To enhance this brain plasticity, the use of Brain-Machine Interfaces (BMI) has been proposed in several studies [13, 14]. In [15], the success rate in the detection of walking intention through cortical signals shows a strong correlation with motivation of stroke patients. Cortical information regarding cognitive mechanisms can be extracted from electroencephalographic (EEG) signals [16, 17, 18]. The proper understanding of these cortical processes is helpful to define a cognitive model of the brain which may be used to modify the parameters of physical therapies. By applying this method, patients will perceive how rehabilitation strategies change according to their cognitive state, increasing their level of involvement and, as a consequence, enhancing the plastic properties of the brain during therapies. According to literature, this process should boost the regeneration of neural paths, which, ultimately, will improve rehabilitation results both in terms of motor function recovery and therapy duration. Walking for SCI patients is cognitively challenging. The attentional demand of gait seems to be an important factor related to motor recovery [19, 20]. Decoding this parameter during gait rehabilitation is helpful to measure functional recovery. The current work is focused on this topic with the final goal of using the attention during gait to modify the assistance provided to SCI patients during lower limb rehabilitation.

It was found that the attention paid on gait is associated to selective attention mechanisms manifested as synchronization and desynchronization of gamma band power in EEG signals [21, 22, 23]. Other works analyze attention mechanisms by analyzing visual or auditive evoked potential while walking feedback is provided [24, 25]. As these potentials depend on how much attention is paid to them, they will change according the attention paid to gain instead of the stimulus. In [26], easy and hard mathematical operations are presented to subjects while walking. But, as in the other works, it is only indicated that significant differences are found, and not success rates are provided. In this regard, an offline analysis was previously performed in [27] to evaluate how attentional demands affect cortical potentials during gait. Offline results for healthy participants and SCI patients provided an average of 67% of success rate for 4 attentional tasks during walking.

The purpose of this work is the development of an online system based on the offline research performed in [27]. The final system provides an attention index between 0 (lowest) and 1 (highest). The development of this system faces three critical points. The first one is the adaptation of the offline algorithms to fit specific time processing restrictions associated to real time systems. To enhance brain plasticity, patients have to experience a direct relationship between the rehabilitation therapy and their cognitive state [28]. In this work, real time is defined as those processing and classification time conditions needed to analyze an incoming epoch before the following epoch is acquired. The second point is related to the reliability of the measured EEG signals. The volume conduction of the scalp induces the appearance of undesired signals from non-cortical sources coupled to EEG channels [29]. These artifacts come from different sources (physiological, environmental, etc. [30, 31, 32]) and it has been proved that their influence on EEG signals increases under heavy movement conditions [33]. Moreover, in a previous work [34], it was shown that, during walking, EEG signals are significantly affected by conductivity changes produced in the electrodes. These changes were related to displacements in the circuit formed by the electrodes, the conductive gel and the scalp. The specific head movements performed during ambulation were directly associated to the scalp areas affected by these noises. To avoid misleading results related to artifact appearance it is necessary to design an artifact detection algorithm to identify and reject polluted trials. The final aspect evaluated in this work is the amount of data needed during the creation of the classification model and the stability of its performance during time. Modeling techniques have been widely studied for EEG analysis in order to increase BCIs performance [35, 36, 37]. The time variability of EEG signals is a recurrent issue in modeling. It implies a decrease in the performance of classification associated to the time that has passed from the moment the model was created [38]. In this work, EEG signals are standardized prior to model creation to increase the similarities of the signals acquired in different dates. Moreover, the performance of the model regarding classification is tested with EEG data registered on different days. The final system has been validated with healthy participants and incomplete SCI patients.

2. Material and Methods

2.1. Data Acquisition

EEG data were recorded using 31 active electrodes located on the scalp with the following distribution: Fz, FC5, FC1, FC3, FCz, FC2, FC4, FC6, C5, C3, C1, Cz, C2, C4, C6, CP5, CP3, CP1, CPz, CP2, CP4, CP6, P3, P1, Pz, P2, P4, PO7, PO3, PO4 and PO8 according to the international system 10/10. The ground was located in AFz position and all channels were referred to an electrode firmly located on the right earlobe through a grip. Electrical signals were sent through a small wifi transmitter to a commercial amplifier (actiCHamp, BrainProducts, GmbH, Germany) where they were digitalized using a sampling frequency of 500 Hz. In addition, a hardware band-pass filter between 0.5 and 100 Hz was applied to remove the spectral information beyond the bandwidth of cortical signals and a 50-Hz Notch filter was used to remove the power line interference.

2.2. Processing

To design an online real time system, it was necessary to set certain time restrictions during the signal processing. During gait rehabilitation, the attentional demands experienced by users do not present quick variations in short time periods. For that reason, it was decided to design a system that provides a value of the attention coefficient each 0.5 seconds. To obtain this result, the system developed was capable of processing the incoming data and taking a decision in less than 0.5 seconds. After that, it waited until the following 0.5 seconds of data were acquired to repeat the process.

Each 0.5 seconds, a new epoch went under the processing stage. In order to have enough time information, the epoch length was selected as 1 second. From that length, the last 0.5 seconds corresponded to the newest acquired data and the remaining 0.5 seconds were selected as an overlap of the previous processed epoch (Fig 1A). On each iteration of the real time acquisition loop, the raw data registered were presented as a 31×500 matrix (31 channels and 500 samples).

The Common Average Reference (CAR) method was applied to each channel by subtracting the average value of the remaining set of channels (Fig 1B) [39].

Then, prior to spectral computation, it was necessary to apply a standardization algorithm capable of moving to the same amplitude range all the registered signals, from different users and days, in order to made them statistically comparable. However, it is important to reduce, to its minimum, the loss of information associated to the standardization process. In the current work, sig-

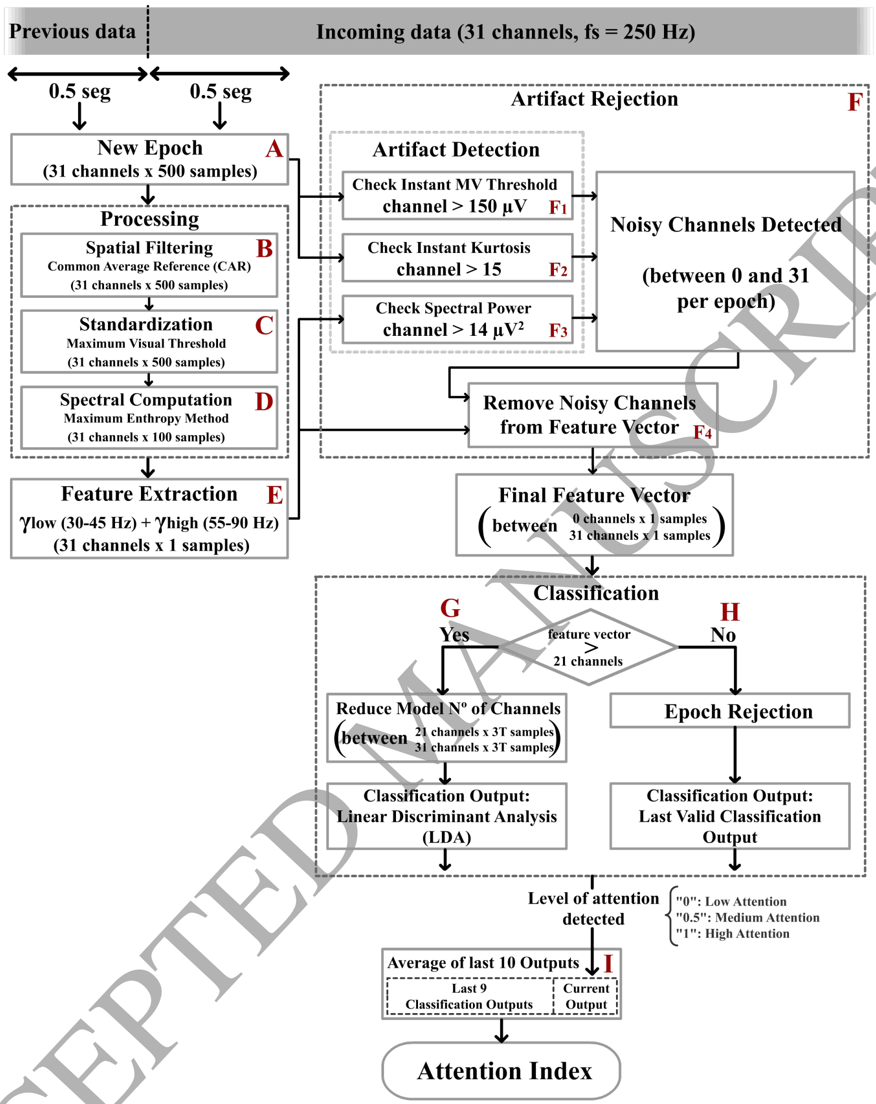

Figure 1: **Signal processing and classification.** Block diagram of the processes applied to each new incoming epoch regarding processing, artifact removal and classification. As a final result, the instantaneous attention index was obtained.

nals were standardized using their Maximum Visual Threshold (MV Threshold in Fig 1C). This parameter was introduced in a previous work [27]. It uses information from the N-previous data epochs. X matrix symbolize electrodes as rows and time steps as columns, therefore, X[e, t] represents the potential at electrode 'e' and time point 't'. The MV Threshold for the electrode e was computed according to equation 1, where $X^e_{((i-1)\times L+1):(i\times L))}$ is the L-samples epoch ($L = 250$, 0.5 seconds) number i for $i = 1, 2, 3...N$ with N being the total number of previous epochs evaluated.

$$MVThreshold^e = \frac{1}{N}\sum_{i=1}^{N} max(X^e_{((i-1)\times L+1):(i\times L))}) \tag{1}$$

In [27], the MV thresholds were computed during an offline analysis with runs of 160 seconds, however it was proved that after 50 seconds the MV Threshold already converged to its final value. As in the current work each incoming epoch contained 0.5 seconds of new data, the information of 100 epochs ($N = 100$, 50 seconds) was used to compute the MV Threshold for each electrode. This value was computed for the 31 channels at each iteration of the acquisition loop. Results of these computations were used to standardize the signals according to the equation 2, where $V(t)_e$ is the raw EEG signal of the electrode e and $MVThreshold_j$ is the MV Threshold of the channel j, with $j = 1, 2, 3, ...Ch$, being Ch the total number of channels.

$$SV(t)_e = \frac{V(t)_e}{\frac{1}{Ch} \times \sum_{j=1}^{Ch} \times MVThreshold_j} \tag{2}$$

$SV(t)_e$ represents the Standarized V(t) for each electrode e. By averaging the MV Thresholds of the 31 channels, the information provided by the power difference between electrodes was not lost after the standardization. At the same time, it made possible the comparison of signals acquired on different sessions and different users in terms of amplitude.

Standardized signals resulting from these methods were then subjected to an autoregressive spectral analysis through the Maximum Entropy Method (MEM) introduced by Burg in [40]. The AR-parameters were computed by minimizing the sum of the square forward and backward prediction errors [41]. This method highlights the spectral components associated with the highest entropies which are also related to those containing the most relevant information. The spectrum between 1 and 100 Hz was computed for each epoch with a spectral resolution of 1 Hz (Fig 1D).

To evaluate the selective attention mechanisms associated to the gait process it was necessary to extract features that contained information about the synchronizations and desynchronizations produced in the gamma band [21]. Following the results obtained in [27], a combination of γlow (30-45Hz) and $\gamma high$ (55-90Hz) frequencies were summed to get a single feature per electrode. Finally, 31 features per epoch were used as an input for the classification (Fig 1E).

2.3. Artifact Rejection

A common problem during EEG acquisition is the appearance of undesired signals that cover the potentials under research. These artifacts are even more critical on experiments performed during ambulation [33]. In addition, for online artifact removal techniques, it is not possible to use neither future signal values (as they are not registered yet) nor huge amount of past data (as there are processing time limitations related to the real time conditions). In the current work, to avoid misleading results related to the appearance of artifacts, 3 parameters were evaluated during single epoch processing to detect noisy electrodes (Fig 1F).

Prior to standardization, the instant value of the Maximum Visual Threshold was computed for every electrode of the epoch under analysis. These values represent the maximum amplitude measured for each epoch. All electrodes that exceed 150 μV were considered noisy (Fig $1F_1$). This decision was made after evaluating the typical range of EEG amplitudes, which is between 0.5 and 100 μV according to [42] and our previous work [34].

In addition, during this stage, the kurtosis of all electrodes was computed. This parameter, related to signal variability, provides a measure associated with the appearance of heavy tails in the signals [43]. For that reason, it has been widely used to detect unexpected EEG signal variations mostly associated to blinks and similar low frequency potentials [44, 45, 46]. The threshold is based on standard deviation of EEG signals and it was selected to allow that signals with artifacts can be rejected. The value was calculated by using previous offline registers for procedure validation and previous works [34] in which artifacts where visually checked and compare with the other parameters. In the current work, electrodes with kurtosis values higher than 15 were considered noisy (Fig $1F_2$).

Another critical point regarding the artifact appearance was the features extraction. γ band power is associated to changes in the selective attention mechanisms but it is also modulated by EMG signals (usually by those produced near the scalp area like jaw clenches or facial grimacing [47, 48]). However EMG influence could be easily distinguished as it produces significant power changes in γ band compared with EEG signals. After evaluating the influence of these artifacts [34], it was decided to consider noisy those electrodes whose features exceeded 14 μV$^2\cdot$ Hz (Fig $1F_3$).

2.4. Classification

Features vectors were classified using a Linear Discriminant Analysis (LDA) algorithm which is a generalization of Fishers Linear Discriminant classifier [49]. The model used was defined as a $31 \times 3T$ features matrix and a $1 \times 3T$ label vector with 31 being the number of features per trial and T the number of trials per task. Tasks were equally distributed in the model to avoid any tendency in the classification output. The model also contained the initial values of the MV Thresholds used during standardization. These values were updated during online analysis.

Prior to classification, the artifacts detected during processing were evaluated (Fig $1F_4$). At this point, there were 2 different courses of action depending on the number of noisy electrodes appearing on each incoming epoch. If 10 or less electrodes were affected by artifacts (less than the 33% of the epoch information), the rows of the $31 \times 3T$ feature matrix associated with the noisy electrodes were removed from the model and the classification was performed using only clean electrode features (Fig 1G). Otherwise, the epoch was completely rejected and the last valid classification value was used as classifiers output (Fig 1H).

Depending on the task identified, the classifier provided an output for low attention (0), medium attention (0.5) or high attention (1). In order to reduce the influence of false positives, the final attention index provided by the system was obtained after averaging the lasts 10 classification outputs (Fig 1I). The goal of averaging the last 10 epochs was performed in order to obtain a continuous index of the attention level across the time. If the predicted value every 0.5 seconds (0, 0.5 or 1 regarding attention level) is directly used to control a system, even with a high success rate, it will change several times from one level to another due to false positives. Therefore, in order to avoid that, this average allows obtaining a tendency value that show an smooth attention level. It was analyzed several values and 10 epochs was experimentally selected as it was a relatively stable value. With more epochs, the change between one level to other was very slow, and with less epochs the variability was too high when users did not have high success rates.

Additionally, the confusion matrix for the three different levels of attention was computed. This way it can be analyzed, not only the global % success rate, but also which attention levels are detected during each task and how it can affect to the performance of the system.

2.4.1. Chance Level Computation

To validate the classifier performance, it was necessary to confirm the significance between the success rate values obtained and the chance level. Mathematically, the chance level for a 3-task classification system with an infinite number of observations is 33% assuming class equality (which is the case of the current work). However, for a real finite data analysis, the chance level is a range of values around the mathematical value for infinite observations. The upper and lower bounds of this range vary depending on the number of observations classified to obtain a single value of accuracy. The equations used to compute the chance level for the current system were the same used in the previous offline study [27].

2.5. Evaluation metrics

After each run, four parameters related to the performance of the experiment were obtained:

- **Attention index vector:** contains the attention indexes provided for each epoch after the classification stage. Taking into account the segmentation parameters (1-second epochs with 0.5 seconds of overlap) and the length of a run ($30\, s \cdot attentional\, task\; = \; 90s$), the size of this vector was 1x180. After a session (8 runs), the results regarding this parameter were represented as an 8x180 matrix.

- **Success rate:** contains a single value with the percentage of the correctly classified tasks. To compute this parameter, the attention index values were not used, instead, the instantaneous values provided by the classifier for each epoch (0, 0.5 or 1) were compared to the real task performed at each time. After a session (8 runs), a 1x8 success rate vector was obtained.

- **Rejected data:** contains a single value with the percentage of data rejected during a run. After a session (8 runs), a 1x8 vector is provided.

- **Artifact spatial distribution:** contains the number of noisy epochs associated to each acquisition channel (represented as a 1x31 vector). After a session (8 runs), a 8x31 matrix was provided.

2.6. Graphical Interface

A graphical interface was used to provide visual information about the development of the experiment during the online processing. Fig 2 shows the appearance of the interface. Section A shows the attention level measured. Section B represents the average number of electrodes used along the experiment and consequently the data lost (in percentage). In section C, a red bar was used to show the number of electrodes that were used for the classification on each loop iteration. This value provided a measure of the attention index validity at each time instant. Section D shows the evolution of the Maximum

Visual Thresholds of the 31 channels in order to detect unexpected changes in the scalp-electrode conductivity during the experiment [34]. In section E, the scalp with the electrode distribution used during acquisition is represented. The electrodes changed their color (from white to black) following a red shade gradient representing the relationship between the epochs classified and the noisy epochs detected. Finally, section F shows the average success rate obtained on the current run. All sections were updated every 0.5 seconds except for section F (success rate) which was updated only at the end of each run. The parameters shown by the interface during the experiment were saved with the acquired EEG information to check the validity of the final results.

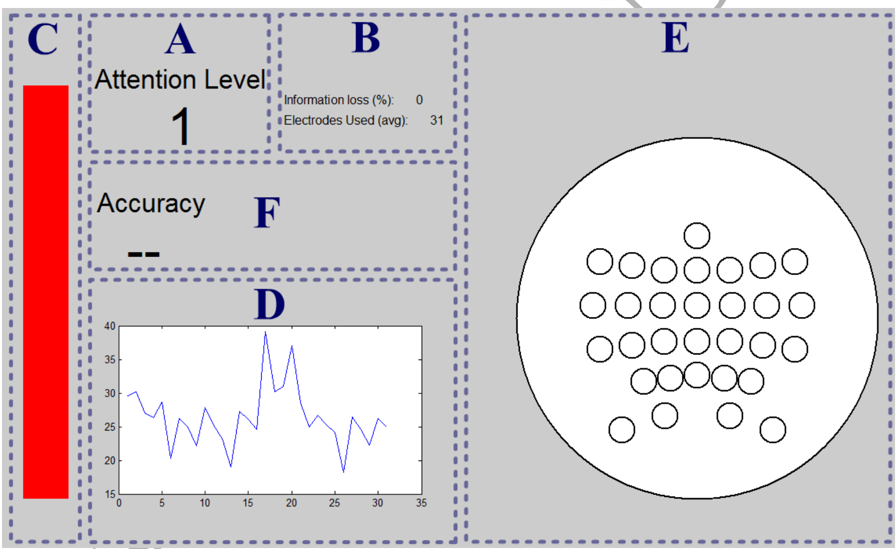

Figure 2: **Graphical interface.** Graphical interface used to provide information about the experiment development. A: instantaneous attention level; B: average of electrodes used and data lost; C: instantaneous electrodes used; D: instantaneous maximum visual threshold of each electrode; E: instantaneous spatial distribution of artifacts detected; F: accuracy at the end of a run.

2.7. Experimental Procedure

Before starting the experiment, participants were instrumented with the EEG acquisition devices. Conductive gel was located in each channel to reduce the impedance between the scalp and the electrode. The experiment was based on a dual task paradigm where participants performed 2 different tasks at the same time. In this case, participants were asked to walk on a treadmill at 2 km/h while they performed other tasks that modify their amount of attention to gait. A run of the experiment was composed of three 30-seconds trials (as shown in Fig 3). On the first trial, participants were asked to mentally solve mathematical operations during gait. The operations were presented through a screen located in front of them. During this task, participants were focusing on a non-gait related task, for that reason it was labeled as low gait attention. For the second trial, participants were asked to walk while looking to the front and no distractions were presented. This task was labeled as medium gait attention. Finally, during the third trial, participants were asked to walk following some marks located in the treadmill with an unsteady gait pattern. Following such pattern made them increase the attention towards the gait process. For that reason, this task was labeled as high gait attention. A session of the experiment was composed of 8 runs.

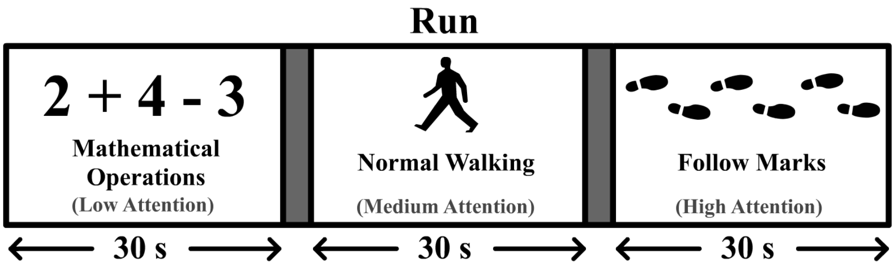

Figure 3: **Run description.** The run was divided into three trials of 30 seconds each. On the first trial the user was asked to perform mathematical operations during gait. On the second one the user was asked to walk normally. And, on the third one, the user was requested to follow several marks located on the treadmill with an unsteady gait pattern. The tasks were labelled respectively as low, medium and high attention during gait, regarding how each one influenced the user's engagement throughout the recording.

2.8. Studies Performed

Healthy participants and patients performed one session of the experiment to validate the performance of the online system. Moreover, healthy participants performed an additional session (two days after the first one) which was used to test the stability of the classification model through time. In Fig 4, a scheme of both sessions is shown. Each session was composed of 8 runs. The experiment ran online from the beginning of the session so it was necessary to define a default classification model for the first run and session. The model was composed of random features, a vector of balanced labels and a set of 31 MV Thresholds (all of them ones). In each subsequent run, a new model was created using the features, labels and MV Thresholds from all the previous runs. This process was repeated until the fifth run (where the model was created with data from the fourth first runs. Then, features and labels were not updated any more. However, the MV thresholds were still being updated during real time processing in order to correct long term amplitude changes in the EEG signals [50]. Last four runs (from 5 to 8) were used to compute the final success rate values for each participant. The second session of the experiment was only performed by healthy users. In this case the model used was the one already created on the previous session. Again, the features and the labels remained constant during the whole session and the MV Thresholds were updated on each iteration of the acquisition loop. In this case, the success rate values obtained during the 8 runs of the second session were used to test the stability of the model after applying the MV Thresholds standardization.

2.9. Participants

Four healthy users performed the experiments, three males and one female with ages between 26 and 30 (27 ± 2) years old. Also four incomplete Spinal Cord Injured (iSCI) patients participated at the experiment, three males and one female with ages between 23 and 66 (44.7 ± 17.6) years old. Healthy participants were graduate, PhD and Postdoc Students from Miguel Hernández University of Elche (Spain) with no known diseases, and patients were recruited from the

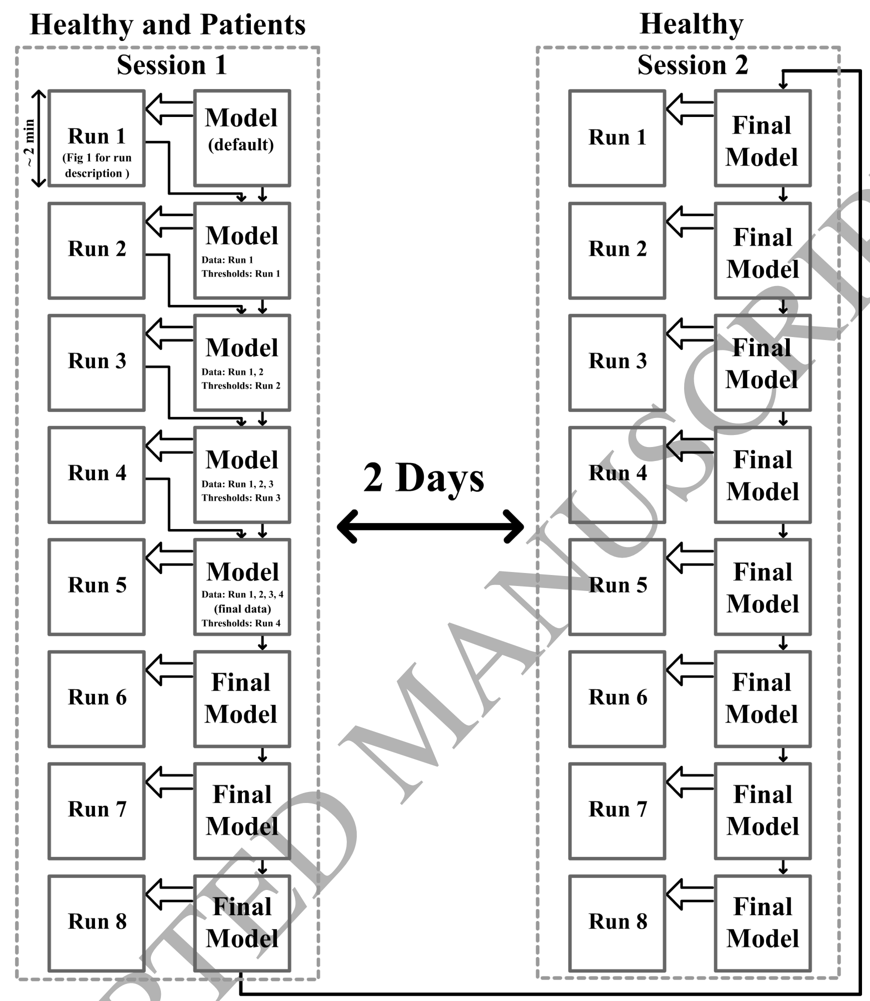

Figure 4: **Experimental protocols.** Block diagram of both sessions performed during this work. On the first session the model was updated using the information of the first 4 runs. After that, the data used to create the model remained constant and the MV Thresholds were updated during real time analysis. This session was performed by healthy participants and iSCI patients. The second session was performed two days after the first using the final model previously obtained. Thresholds were still updated during real time analysis. Only healthy participants performed the second session.

National Hospital for Spinal Cord Injury in Toledo (Spain) with motor lesions between C7 and T10. The patients selected were able to walk by themselves or using simple assistive tools like crutches or walkers. All users were previously informed about the experimental procedure and they signed an informed consent according to the Helsinki declaration. The experimental procedure was approved by the ethics committee of the Miguel Hernández University of Elche (Spain).

3. Results

3.1. Artifact rejection and spatial distribution

The information obtained during the first experiments regarding data rejection is represented on Table 1 for each user. On the two rows, the average amount of rejected data and its standard deviation are shown. Also, the maximum and minimum numbers of noisy epochs rejected for each participant (rows 3 and 5) with the names of the associated electrodes (rows 4 and 6) are provided.

In addition, in Fig 5 the spatial distribution of the noises identified during the experiment are shown for patients and healthy participants. This spatial distribution is represented in two different ways. On the left, the number of noises detected are compared with the total number of epochs (noisy and not noisy) evaluated. This representation shows the influence of noise among all the data acquired during the experiment. In this case it is clear the low amount of electrodes found noisy during the experiments. On the right, the number of noises detected on each electrode are compared with the number of noises detected on the noisiest electrode. In this way, the areas of noise influence are emphasized, so it can be evaluated if the detected noise is related with some specific electrode or if it is not associated to any specific scalp area as the image suggest.

3.2. Classification results

In Fig 6, the average success rate of the system is represented for each participant. In this case, for healthy users it is shown separately session 1 from session 2. For session 1, the success rates of the last 4 runs were averaged, and for the session 2, all 8 runs success rates were averaged. For patients, the

Table 1: **Data lost results.** "Loss (Avg)" and "Loss (Std)" rows show the average and standard deviation (in %) of the data contaminated by artifacts for each subject. Rows "Min Noises" and "Max Noises" show the minimum and maximum number of noisy epochs found in an electrode for each volunteer. Moreover, the name of the electrodes presenting minimum and maximum number of noisy epochs are respectively shown in rows "Elec (Min)" and "Elec (Max)".

	Healthy Subjects				**iSCI Patients**			
Subjects	**H1**	**H2**	**H3**	**H4**	**P1**	**P2**	**P3**	**P4**
Loss (Avg)	0.4%	0.2%	1.3%	0.4%	0.5%	9.1%	7.5%	1.4%
Loss (Std)	0.8%	0.3%	2.1%	0.7%	0.5%	4.9%	5.1%	2.8%
Min Noises	6	2	26	7	2	86	79	14
Elec (Min)	PZ	FC2	PZ	C5	PO7	P2	P2	FC5
	PO3	CZ		CP3	C5			FC3
	CP3	CP1		P1	CP3			C5
		C1						C1
		CPZ						P2
Max Noises	13	17	76	24	13	140	109	31
Elec (Max)	FCZ	PO8	CP6	CP6	FC4	C6	CP1	C6
	PO8							

4 last runs of the first session were used to show the averaged success rates. The standard deviation values are represented with black lines centered on each success rate bar.

First session of healthy users got an average success rate of 77.3±7.6 % while the second session decrease to 69.0±14.4 %. Patients get an average value of 58.0±11.9 %.

The last bar of each group (both sessions of healthy and single session of patients) represents, in terms of average and standard deviation, the chance level computed given our classification system (3 tasks) and the data populations used to computed the final success rates (4 samples for first session of healthy subjects and patients, and 8 samples for second session of healthy subjects). By

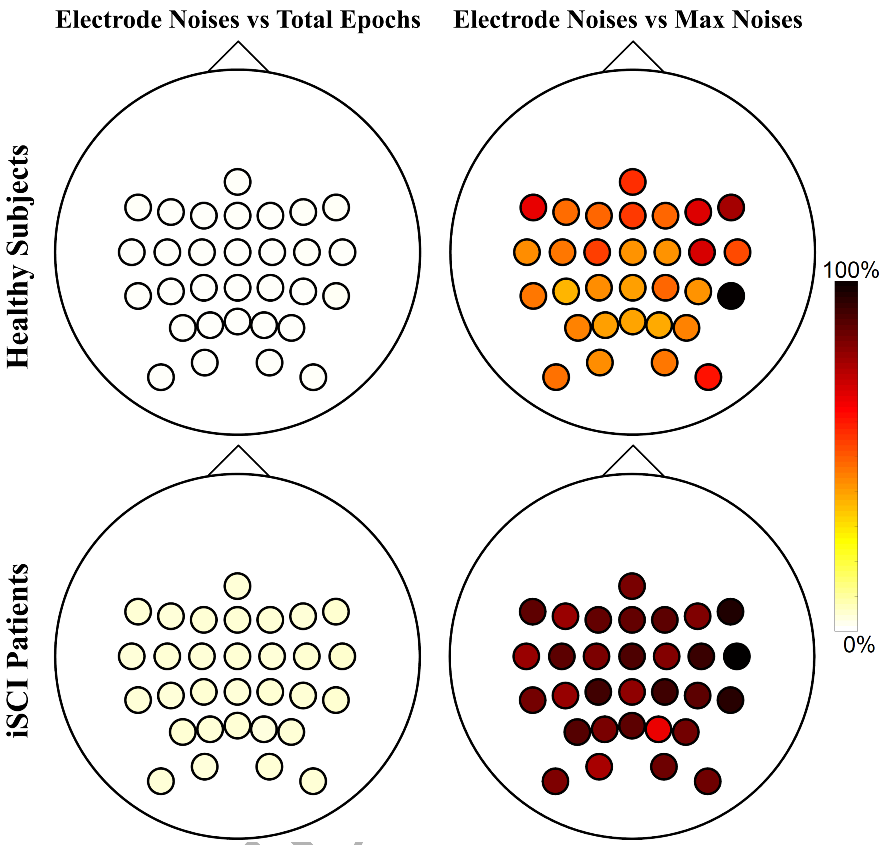

Figure 5: **Noise spatial resolution.** Spatial distribution of noisy epochs detected for healthy subjects and iSCI patients. The first column compare the noisy epochs detected on each electrode to the total amount of epochs processed. The second column compare the noisy epochs of each electrode with those detected in the noisiest electrode. It is represented in percentage from 0% light to 100% dark.

following the procedure explained in [27] and taking into account that chance level for infinite number of observations is 33% for our 3 tasks, it was calculated the chance level for finite number of samples (each sample includes 180 epochs). This imply that for first sessions chance level is 33.4±3.4 and 33.4±2.4 for second session of healthy subjects.

A statistical Wilcoxon Rank-Sum Test with a confidence interval of 95% was applied to evaluate the significance between the each participant and the associated chance level [51]. After applying a Bonferroni correction for multiple comparisons [52], the success rate values that show significant results were marked with an asterisk.

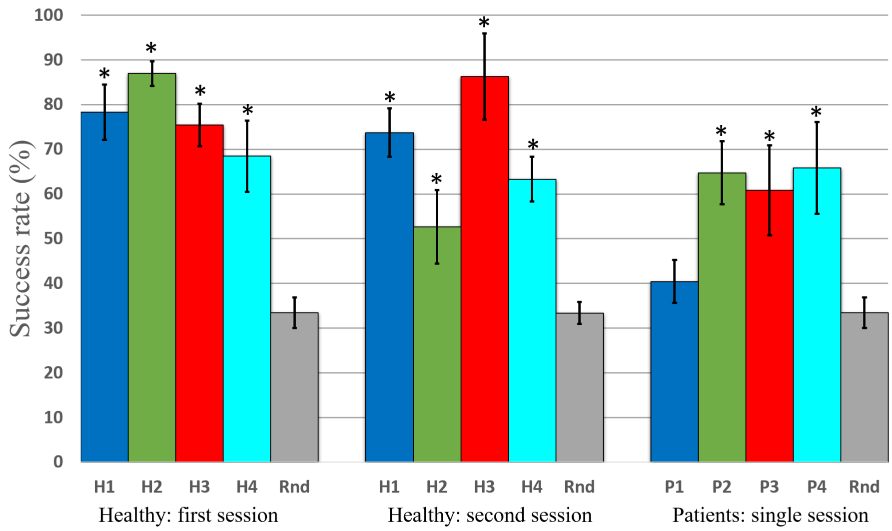

Figure 6: **Classification results.** Average success rate computed for each subject including data from all the runs performed with the final model (4 runs of the first session and 8 of the second for healthy subjects and 4 runs of the first session for iSCI patients. The gray bar represent the chance level of the classification system used. The users whose averaged success rate values show significance against the chance level are marked with an asterisk.

3.3. Model stability through time

There were two important aspects regarding classification performance during model creation. The first one was the amount of data needed to create the model which was directly related to the training time. The second aspect was the performance of the model classifying data acquired on distant time periods. To test these aspects, the success rate values obtained for each run are shown in Fig 7. During runs from 1 to 4 of the first session (both for healthy and patients), the model was updated with the data recorded from previous runs. The success rate values from this session (8 runs) were used to show how the classifier performance evolved when the data used to create the model increased.

Moreover, two days after this session, healthy participants performed a second session of the experiment using the model created during session one. Success rates values obtained from the second session are also shown on Fig 7 for healthy participants. This information provides a measurement of the stability of our classification algorithm through time.

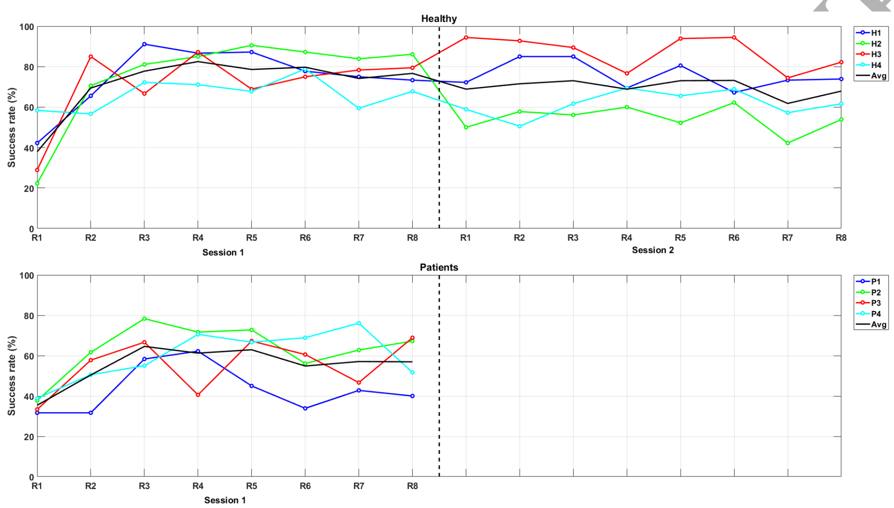

Figure 7: **Success rate evolution.** Success rate individual values for each run of both sessions. Each colored line joins the individual values of a single subject.

3.4. Confusion matrix

Even the global success rate reported in previous sections is high, it should be analyzed how the different requested attention levels are detected related each other. Table 2 shows the confusion matrix for each user. In the case of healthy users it is shown separately first and second session. Each matrix shows the average of all the runs where the final model is used.

On one hand, results show that high attention level is very well detected in all users. Healthy subjects got and averaged success rate of 97% and 83% for each session respectively, and patients got also a suitable value of 86%. On the other hand, low attention level is also usually properly detected. For healthy subjects a success rate of 84% and 80% respectively are obtained. For patients results show worst performance getting an average 41%. Low level is confused with medium and high attention levels. Finally, medium attention level is the one that got lower accuracy as it is usually confused with low attention level. In this case all users got success rates near 50%.

3.5. Attention index evolution

Finally, fig 8 shows the average attention index for each participant. For healthy users, the values were obtained averaging 12 runs (the last 4 runs from the first session and 8 runs from the second session). On the other hand, for patients, the values were obtained averaging the last 4 runs of the first and only session. The attention index of each participant was represented with a colored dotted line. In addition, a black straight line represented the average value of the index for the whole set of healthy users and patients, respectively. The vertical black dotted lines delimited the X-axis according to the real attention level. In an ideal performance of the system, the attention index should be 0, 0.5 and 1 for low, medium and high attention level, respectively.

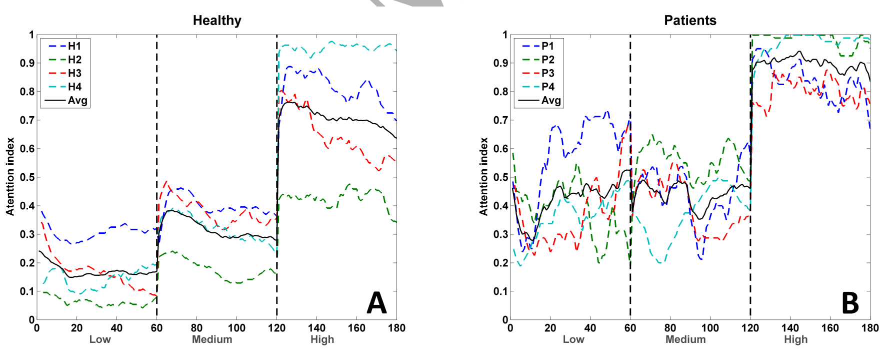

Figure 8: **Attention index evolution.** Average attention index computed for each subject including data from all the runs performed with the final model (4 runs of the first session and 8 of the second for healthy subjects and 4 runs of the first session for iSCI patients).

Table 2: **Confusion matrix.** Averaged confusion matrix for each user is shown. For first session of healthy (first column) and patients (last column), averaged confusion matrix for runs 5 to 8 (when final model is set) for each user are shown. Moreover, average confusion matrix of the 8 runs of session 2 of healthy subjects is shown in center column.

Real attention level performed

Predicted attention level

	H1 session 1			**H1 session 2**			**P1 session 1**		
	L	M	H	L	M	H	L	M	H
L	**96.3**	60.8	0.4	**96.9**	63.7	5.6	**32.9**	46.7	13.3
M	3.8	**39.2**	0.0	3.1	**36.3**	0.0	13.8	**14.2**	12.5
H	0.0	0.0	**99.6**	0.0	0.0	**94.4**	53.3	39.2	**74.2**

	H2 session 1			**H2 session 2**			**P2 session 1**		
	L	M	H	L	M	H	L	M	H
L	**75.8**	15.0	0.0	**88.1**	65.2	59.6	**57.1**	23.8	1.7
M	24.2	**85.0**	0.0	11.9	**34.6**	0.2	12.1	**39.2**	0.4
H	0.0	0.0	**100.0**	0.0	0.2	**40.2**	30.8	37.1	**97.9**

	H3 session 1			**H3 session 2**			**P3 session 1**		
	L	M	H	L	M	H	L	M	H
L	**99.2**	69.6	2.1	**89.0**	23.3	4.2	**45.4**	30.4	14.6
M	0.8	**29.2**	0.0	10.8	**75.4**	0.2	33.3	**62.9**	11.2
H	0.0	1.3	**97.9**	0.2	1.3	**97.5**	21.3	6.7	**74.2**

	H4 session 1			**H4 session 2**			**P4 session 1**		
	L	M	H	L	M	H	L	M	H
L	**66.3**	49.2	0.4	**45.0**	26.9	0.0	**26.7**	26.2	0.0
M	33.8	**49.6**	10.0	32.7	**40.2**	0.0	72.1	**73.8**	2.9
H	0.0	1.3	**89.6**	22.3	32.9	**100.0**	1.3	0.0	**97.1**

4. Discussion

Results show differences in the amount of data rejected depending on participants conditions (see Table 1). Rejected data from patients (4.6±1.9%) is significantly higher than data rejected from healthy participants (0.6±0.5%). The spatial representation of artifacts in Fig 5 also supports these results. For healthy participants, it is not appreciable the level of contamination as it is very low compared to the total amount of data evaluated. However, for patients, the electrodes present an appreciable level of contamination. This is also an expected result as patients walking patterns are more susceptible to the appearance of motion artifacts. On the other hand, the artifacts appearance does not seem associated to any specific scalp area (Table 1). This can be seen more clearly in the spatial representation of artifacts in Fig 5, where all the electrodes present similar amounts of contamination.

Although the attention index for a specific task shows moderated deviations between healthy subjects, the differences between low, medium and high attention levels are easily distinguished within the attentional range associated to a single participant (Fig 8A). Similar results are obtained for incomplete SCI patients except that, low and medium attention levels do not present significant differences (Fig 8B). These results are consistent with the confusion matrix obtained (Table 2) where high and low attention level got higher success rates while medium attention level is more confuse with the other levels. The global success rates obtained on Fig 6 support these results as patients show lower success rate values (58.0±11.9%) than healthy subjects (77.3±7.6%). The success rates of every user (except for patient P1) show significant differences compared to the chance level computed for the current classification system. This behavior fits the findings in [27] where patients show less class separability due to the inherent difficulties they experience when they try to reduce their attention on gait during low attentional tasks.

Regarding classification performance, the success rate values obtained during the first session of the experiment present a relevant increase during the first three runs (Fig 7). On the first run, success rates are in the range of chance level as the model at this point was created with default random data. After the third run, success rates do not experience huge variability and their values have significant differences compared to chance level. These are the expected results as the model used during session one is updated during the first four runs. In fact, it seems that updating the model after the third run does not improve the classification performance. Results for both healthy subjects and patients present similar behaviors. Moreover, success rates obtained during the second session performed by healthy subjects (Fig 7) show a decrease of 8.3% in the averaged performance (69.0% of averaged success rate). However, for all subjects (except H2), results are above chance level and they presented small variability across the session. These results show that the use of the MV Threshold as standardization parameter provides higher model stability during data classification on different days. The biggest reason for the reduction of the results in the experiments of the second session is because the model is kept. Even some users get suitable results, in order to improve results for all users, future works will assess a new very short training in second session. The model will be created using this new training and the data of the experiments performed in the first session. This way, it is expected that with only a couple of minutes of training, results can be similar to the obtained in the first session. These results suggest that it is possible to properly detect low attention level from high attention level with high performance. In order to properly detect other intermediate attention levels the continuous attention level index can be used to analyze the tendency of user's attention.

There are not similar works that offer success rates that help to compare the performance of our development. Only [26] performs an study where mathematical operations are performed while walking and it concludes that significant differences are found, but not success rates are provided. In this regard, a comparison with our previous work [27] where 4 attention levels are evaluated during gait. In this work 12 healthy subjects obtain a 69% of success rate while patients got a 57%. In the current work, not only the results have been improved, but also attention level is evaluated in real time.

This paper validate the system in a more realistic condition for a rehabilitation therapy where the attention level index need to be obtained in real time. It has verified that both healthy and patients generate the continuous attention level index showing a high tendency to the requested level. During a rehabilitation therapy is desirable that patients be as more center as possible in their gait. Therefore, if an exoskeleton is used for gait rehabilitation, the index can be used to modify the level of assistance of the exoskeleton. If the user have high attention, the pattern of the exoskeleton will help the patient. In the case the index decreases due a low attention level, the pattern will be adapted to allow obtaining again a high attention level. This will allow the patient to always keep a good involvement during the therapy increasing its rehabilitation results. This index can also be used to determine if the therapy applied should be modified in order to be less bored and more participative, always for improving the involvement of the user. Moreover, it can be a good resource for medical staff to know how well therapies work. It is also important to remark that the designed system adjust the model only until run 4. This implies a reduced training time that allow starting with the therapy sooner. Moreover, the relevant results of the second session will allow that a new training not be necessary. In this work, subjects continue performing task to reduce or increase the attention level in order to evaluate the behavior of the system. But in a real experiment, after the initial training, subjects will not need to continue performing these kind of tasks. They will directly perform the therapies while their attention levels are obtained in real time.

5. Conclusion

In this work, an online system to measure the attention level during gait has been developed from a prior offline study [27]. The final system provides an attention index between "0" (lowest attention) and "1" (highest attention) every 0.5 seconds during human gait. The system has been validated with 4 healthy subjects and 4 incomplete SCI patients providing an average success rate of 68.1% in the classification. The attention level classified shows more separability for healthy subjects (77.3%) than for patients (58.0%). The amount of data contaminated by motion artifacts have been measured showing significant differences between patients (4.6%) and healthy subjects (0.6%). Also, polluted electrodes are spatially distributed randomly for both patients and healthy participants. Finally, the success rate values are stable during a single session and present a decrease of 8.3% (success rate of 69.0%) when the classification is performed 2 days after the model was created. In both cases, the results show significance against chance level proving the benefits of the parameter used during standardization (MV Threshold).

This work sets the basis for using the attention paid on gait to modify lower limb rehabilitation therapies. On future works, the online classification system developed should be tested during exoskeleton-supported gait to evaluate new possible sources of artifacts induced under this condition. After that, both systems should be tested with a higher population of patients to assure the confidence provided by the system under those circumstances. Finally, the attention levels will be used to modify the level of assistance provided by the exoskeleton. A decrease in patient attention denotes a higher automation of the gait process. To involve the patient in a cognitive way, the assistance should be gradually reduced following the decrement of the attention until the patient does not need assistance to walk. To prove this hypothesis, the integrated exoskeleton-BMI system should be tested with a number of patients and the results in terms of functional recovery should be compared with a control population formed by patients using traditional rehabilitation.

6. Acknowledgments

This research has been funded by the Commission of the European Union under the BioMot project - Smart Wearable Robots with Bioinspired Sensory-Motor Skills (Grant Agreement number IFP7-ICT- 2013-10-611695)

References

[1] W. H. O. (WHO), et al., World report on disability. (2013).

[2] G. Scivoletto, B. Morganti, P. Ditunno, J. Ditunno, M. Molinari, Effects on age on spinal cord lesion patients' rehabilitation, Spinal Cord 41 (8) (2003) 457–464.

[3] D. J. Edwards, On the understanding and development of modern physical neurorehabilitation methods: robotics and non-invasive brain stimulation, Journal of neuroengineering and rehabilitation 6 (1) (2009) 1.

[4] R. Crevenna, Physical medicine and rehabilitationa relevant interdisciplinary speciality, Wiener Medizinische Wochenschrift (2016) 1–2.

[5] M. Confalonieri, P. Tomasi, M. Depaul, G. Guandalini, M. Baldessari, D. Oss, F. Prada, A. Mazzalai, M. Da Lio, M. De Cecco, Neuro-physical rehabilitation by means of novel touch technologies, Stud Health Technol Inform 189 (2013) 158–163.

[6] T. Elbert, C. Pantev, C. Wienbruch, B. Rockstroh, E. Taub, Increased cortical representation of the fingers of the left hand in string players, Science 270 (5234) (1995) 305.

[7] M. A. Lebedev, G. Mirabella, I. Erchova, M. E. Diamond, Experience-dependent plasticity of rat barrel cortex: redistribution of activity across barrel-columns, Cerebral Cortex 10 (1) (2000) 23–31.

[8] A. S. Choe, V. Belegu, S. Yoshida, S. Joel, C. L. Sadowsky, S. A. Smith, P. C. van Zijl, J. J. Pekar, J. W. McDonald, Extensive neurological recovery from a complete spinal cord injury: a case report and hypothesis on the role of cortical plasticity, Frontiers in human neuroscience 7 (2013) 290.

[9] J. Beauparlant, R. van den Brand, Q. Barraud, L. Friedli, P. Musienko, V. Dietz, G. Courtine, Undirected compensatory plasticity contributes to neuronal dysfunction after severe spinal cord injury, Brain 136 (11) (2013) 3347–3361.

[10] S. J. Harkema, Neural plasticity after human spinal cord injury: application of locomotor training to the rehabilitation of walking, The Neuroscientist 7 (5) (2001) 455–468.

[11] M. Bruehlmeier, V. Dietz, K. Leenders, U. Roelcke, J. Missimer, A. Curt, How does the human brain deal with a spinal cord injury?, European Journal of Neuroscience 10 (12) (1998) 3918–3922.

[12] Z. Ying, R. R. Roy, V. R. Edgerton, F. Gómez-Pinilla, Exercise restores levels of neurotrophins and synaptic plasticity following spinal cord injury, Experimental neurology 193 (2) (2005) 411–419.

[13] E. Leach, P. Cornwell, J. Fleming, T. Haines, Patient centered goal-setting in a subacute rehabilitation setting, Disability and rehabilitation 32 (2) (2010) 159–172.

[14] F. Nijboer, N. Birbaumer, A. Kubler, The influence of psychological state and motivation on brain–computer interface performance in patients with amyotrophic lateral sclerosis–a longitudinal study, Frontiers in neuroscience 4 (2010) 55.

[15] A. I. Sburlea, L. Montesano, R. C. de la Cuerda, I. M. A. Diego, J. C. Miangolarra-Page, J. Minguez, Detecting intention to walk in stroke patients from pre-movement eeg correlates, Journal of neuroengineering and rehabilitation 12 (1) (2015) 1.

[16] W. Klimesch, Eeg alpha and theta oscillations reflect cognitive and memory performance: a review and analysis, Brain research reviews 29 (2) (1999) 169–195.

[17] C. S. Herrmann, Human eeg responses to 1–100 hz flicker: resonance phenomena in visual cortex and their potential correlation to cognitive phenomena, Experimental brain research 137 (3-4) (2001) 346–353.

[18] E. Başar, C. Başar-Eroğlu, S. Karakaş, M. Schürmann, Are cognitive processes manifested in event-related gamma, alpha, theta and delta oscillations in the eeg?, Neuroscience letters 259 (3) (1999) 165–168.

[19] Y. Lajoie, H. Barbeau, M. Hamelin, Attentional requirements of walking in spinal cord injured patients compared to normal subjects, Spinal Cord 37 (4) (1999) 245–250.

[20] H. Harbeau, J. Fung, A. Leroux, M. Ladouceur, A review of the adaptability and recovery of locomotion after spinal cord injury, Progress in brain research 137 (2002) 9–25.

[21] T. Gruber, M. M. Müller, A. Keil, T. Elbert, Selective visual-spatial attention alters induced gamma band responses in the human eeg, Clinical neurophysiology 110 (12) (1999) 2074–2085.

[22] J. Fell, G. Fernandez, P. Klaver, C. E. Elger, P. Fries, Is synchronized neuronal gamma activity relevant for selective attention?, Brain Research Reviews 42 (3) (2003) 265–272.

[23] S. Ray, E. Niebur, S. S. Hsiao, A. Sinai, N. E. Crone, High-frequency gamma activity (80–150hz) is increased in human cortex during selective attention, Clinical Neurophysiology 119 (1) (2008) 116–133.

[24] D. Ming, Y. Xi, M. Zhang, H. Qi, L. Cheng, B. Wan, L. Li, Electroencephalograph (eeg) signal processing method of motor imaginary potential for attention level classification, in: 2009 Annual International Conference of the IEEE Engineering in Medicine and Biology Society, IEEE, 2009, pp. 4347–4351.

[25] I. Killane, G. Browett, R. B. Reilly, Measurement of attention during movement: Acquisition of ambulatory eeg and cognitive performance from

healthy young adults, in: 2013 35th Annual International Conference of the IEEE Engineering in Medicine and Biology Society (EMBC), IEEE, 2013, pp. 6397–6400.

[26] E. P. Shaw, J. C. Rietschel, B. D. Hendershot, A. L. Pruziner, M. W. Miller, B. D. Hatfield, R. J. Gentili, Measurement of attentional reserve and mental effort for cognitive workload assessment under various task demands during dual-task walking, Biological psychology 134 (2018) 39–51.

[27] Á. Costa, E. Iáñez, A. Úbeda, E. Hortal, A. J. Del-Ama, Á. Gil-Agudo, J. M. Azorín, Decoding the attentional demands of gait through eeg gamma band features, PloS one 11 (4) (2016) e0154136.

[28] R. J. Siegert, W. J. Taylor, Theoretical aspects of goal-setting and motivation in rehabilitation, Disability and rehabilitation 26 (1) (2004) 1–8.

[29] J. Holsheimer, B. Feenstra, Volume conduction and eeg measurements within the brain: a quantitative approach to the influence of electrical spread on the linear relationship of activity measured at different locations, Electroencephalography and clinical neurophysiology 43 (1) (1977) 52–58.

[30] S. Muthukumaraswamy, High-frequency brain activity and muscle artifacts in meg/eeg: a review and recommendations, Frontiers in human neuroscience 7 (2013) 138.

[31] T. C. Ferree, P. Luu, G. S. Russell, D. M. Tucker, Scalp electrode impedance, infection risk, and eeg data quality, Clinical Neurophysiology 112 (3) (2001) 536–544.

[32] A. J. Shackman, B. W. McMenamin, H. A. Slagter, J. S. Maxwell, L. L. Greischar, R. J. Davidson, Electromyogenic artifacts and electroencephalographic inferences, Brain topography 22 (1) (2009) 7–12.

[33] J. E. Kline, H. J. Huang, K. L. Snyder, D. P. Ferris, Isolating gait-related movement artifacts in electroencephalography during human walking, Journal of neural engineering 12 (4) (2015) 046022.

[34] Á. Costa, R. Salazar-Varas, A. Úbeda, J. M. Azorín, Characterization of artifacts produced by gel displacement on non-invasive brain-machine interfaces during ambulation, Frontiers in neuroscience 10 (2016) 60.

[35] J. Pardey, S. Roberts, L. Tarassenko, A review of parametric modelling techniques for eeg analysis, Medical engineering & physics 18 (1) (1996) 2–11.

[36] F. Wendling, F. Bartolomei, Modeling eeg signals and interpreting measures of relationship during temporal-lobe seizures: an approach to the study of epileptogenic networks., Epileptic disorders: international epilepsy journal with videotape (2001) 67–78.

[37] A. Subasi, Eeg signal classification using wavelet feature extraction and a mixture of expert model, Expert Systems with Applications 32 (4) (2007) 1084–1093.

[38] F. Lotte, M. Congedo, A. Lécuyer, F. Lamarche, B. Arnaldi, A review of classification algorithms for eeg-based brain–computer interfaces, Journal of neural engineering 4 (2) (2007) R1.

[39] D. J. McFarland, L. M. McCane, S. V. David, J. R. Wolpaw, Spatial filter selection for eeg-based communication, Electroencephalography and clinical Neurophysiology 103 (3) (1997) 386–394.

[40] B. Rainford, G. Daniell, μsr frequency spectra using the maximum entropy method, Hyperfine Interactions 87 (1) (1994) 1129–1134.

[41] H. F. Schels, R. Haberl, G. Jilge, P. Steinbigler, G. Steinbeck, Frequency analysis of the electrocardiogram with maximum entropy method for identification of patients with sustained ventricular tachycardia, IEEE transactions on biomedical engineering 38 (9) (1991) 821–826.

[42] M. Teplan, Fundamentals of eeg measurement, Measurement science review 2 (2) (2002) 1–11.

[43] L. T. DeCarlo, On the meaning and use of kurtosis., Psychological methods 2 (3) (1997) 292.

[44] M. A. Sovierzoski, F. I. Argoud, F. M. de Azevedo, Identifying eye blinks in eeg signal analysis, in: 2008 International Conference on Information Technology and Applications in Biomedicine, IEEE, 2008, pp. 406–409.

[45] H. Nolan, R. Whelan, R. Reilly, Faster: fully automated statistical thresholding for eeg artifact rejection, Journal of neuroscience methods 192 (1) (2010) 152–162.

[46] J. T. Gwin, K. Gramann, S. Makeig, D. P. Ferris, Electrocortical activity is coupled to gait cycle phase during treadmill walking, Neuroimage 54 (2) (2011) 1289–1296.

[47] I. I. Goncharova, D. J. McFarland, T. M. Vaughan, J. R. Wolpaw, Emg contamination of eeg: spectral and topographical characteristics, Clinical neurophysiology 114 (9) (2003) 1580–1593.

[48] M. Fatourechi, A. Bashashati, R. K. Ward, G. E. Birch, Emg and eog artifacts in brain computer interface systems: A survey, Clinical neurophysiology 118 (3) (2007) 480–494.

[49] A. J. Izenman, Linear discriminant analysis, in: Modern Multivariate Statistical Techniques, Springer, 2013, pp. 237–280.

[50] Y. Cao, W.-w. Tung, J. Gao, V. A. Protopopescu, L. M. Hively, Detecting dynamical changes in time series using the permutation entropy, Physical Review E 70 (4) (2004) 046217.

[51] W. Haynes, Wilcoxon rank sum test, in: Encyclopedia of Systems Biology, Springer, 2013, pp. 2354–2355.

[52] E. W. Weisstein, Bonferroni correction.

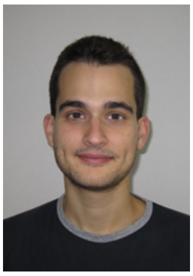

Alvaro Costa García is a research scientist at the Intelligent Behavior Control Unit, BSI, RIKEN. He received M.S. degree in Telecommunications Engineering from the Systems Engineering and Automation Department at the Miguel Hernández University of Elche, Spain (2013). He obtained a PhD in the Program on Industrial and Telecommunications Technology from the same university in 2016. During the PhD, his research was focused on lower limb rehabilitation methods and the study of cognitive mechanisms related to gait through the evaluation of electroencephalographic signals. Currently, he is studying the neural processes behind voluntarily motor control through the evaluation of electromyography and its applications in the field of neuro rehabilitation.

Eduardo Iáñez is a scientific researcher in the Brain-Machine Interface Systems Lab at Miguel Hernández University of Elche (Spain). He holds an M.Sc in Telecommunication Engineering from the Miguel Hernández University of Elche in 2007 and a Ph.D. in Communication and Industrial Technologies by the Miguel Hernández University of Elche in 2012. He has been a visiting researcher at Visiting Researcher at Intelligent Behavior Control Unit, Center for Brain Science (CBS), CBS-Toyota Collaboration Center (BTCC), RIKEN, Nagoya, Japan. His current research interests are Brain-Machine Interfaces, Neuro-robotics and Rehabilitation Robotics. The study of other physiological signals such as ocular or electromiographic are also of interest to improve rehabilitation therapies. http://bmi.edu.umh.es/

Antonio Jos del-Ama started his research career on 2006 at the Biomechanics and Assistive Technology Unit of the National Hospital for Paraplegics, and become its Group Leader on 2017. His research includes biomechanics of motor function, rehabilitation robotics and evaluation of assistive technologies in four research lines: 1) movement analysis, 2) lower limb wearable robotic exoskeleton design, 3) hybrid robot-neuroprosthesis design, and 4) functional evaluation of assistive technology for walking. He has been researcher in several competitive regional, national and European projects related to lower limb wearable robots for walking assistance as researcher and coordinating research activities at partner level. In 2011 he was awarded with the Technological Innovation Award from the Rodolfo Benito Samaniego Foundation for its work on the biomechanical assessment of manual wheelchair propulsion. Between 2008 and 2012 he made a part-time stay in the Neural Engineering Group at CSIC (formerly the BioEngineering Group), getting his PhD in the area of hybrid lower limb exoskeletons for walking assistance. Resulting from this stay, a joint line of research was structured through several National and EU projects (Rehabot, Hyper, BioMot, Extend) From 2015 he is also Assistant Professor at Castilla-La Mancha and Rey Juan Carlos Universities, teaching subjects related with Advanced Electronic Instrumentation and Control, and directed several Bachelors and Master Thesis. From 2012 he is also member of the Commission of Medical and Health Engineering of the Association of Industrial Engineers of Madrid.

Medical Doctor and Ph.D degree obtained in the Faculty of Medicine, Universidad Complutense (Madrid, Spain) with a doctoral thesis about manual wheelchair propulsion ergonomics in spinal cord injury patients (2009). Clinical practice in different hospitals since 1993 as Physical Medicine and Rehabilitation specialist. Researcher from 1994 to 1996 in Institute of Biomechanics in Valencia (IBV). Coordinator of Biomechanics and Technical Aids Department in National Hospital for Spinal Cord Injury (Toledo, Spain) since 2005. Current research focuses on the application of biomechanics to the development of systems based on virtual reality for upper limb rehabilitation treatment and the development of neuro-robotic and neuro-prosthetics to compensate or restore movement disorders. Coordinator of the scientific committee of the Spanish Federation for Disabled Sports from 1998 to 2004. Prseident of AITADIS (Iberoamerican Association of Disabilty Support Technologies).

Jose M. Azorín is the Director of the Brain-Machine Interface Systems Lab and Full Professor of the Systems Engineering and Automation Department at Miguel Hernández University of Elche (Spain). He holds a M.Sc in Computer Science from the University of Alicante (1997, Spain) and a Ph.D. in Robotics (Award for the Best Thesis of the Department) by the UMH (2003, Spain). He has been a visiting professor at the University of Houston (USA) and at Imperial College London (United Kingdom). His current research interests are Brain-Machine Interfaces, Neuro-robotics and Rehabilitation Robotics. Over the last years, his research has been funded by prestigious grants from the European Union and other Spanish government agencies. He has been the PI of more than 10 research projects, and his research has resulted in more than 150 technical papers and 3 patents. Currently, he is a Distinguished Lecturer of the IEEE Systems Council. http://bmi.edu.umh.es/portfolio-item/jose-m-azorin/ http://bmi.edu.umh.es/